International Journal of Fluid Machinery and Systems
Vol. 6, No. 3, July-September 2013

DOI: 10.5293/IJFMS.2013.6.3.121
ISSN (Online): 1882-9554

Original Paper

Hexagonal reciprocating pump: advantages and weaknesses

Milan Stanko and Michael Golan

Department of Petroleum Engineering, NTNU University
S.P. Andersens vei 15 A, Trondheim, 7033, Norway, milan.stanko@ntnu.no

Abstract

This paper reports the 1-D fluid transient simulation results of the discharge flow conditions in a 6-cylinder reciprocating slurry pump. Two discharge manifold configurations are studied comparatively; a case with a hexagon shaped discharge manifold where each cylinder discharges at a single vertex, and a case where all the cylinders discharges are lumped together into a tank shaped manifold. In addition, the study examines the effect of two pulsation mitigation measures in the case of hexagonal manifold; a single inline orifice in one of the hexagon sides and a volumetric dampener at the manifold outlet. The study establishes the pressure and flow fluctuation characteristics of each configuration and decouples the pulsation characteristics of the pump and the discharge manifold.

Keywords: Hexagonal piston pump, pressure pulsation, reciprocating piston pump.

1. Summary

Reciprocating pumps produce flow variations in their discharge end that may excite severe pressure pulsation in their discharge manifolds and piping systems. Therefore, developing of new designs of such pumps or introduction of novel configurations of discharge manifold warn an investigation of their flow dynamic characteristics and their susceptibility to acoustic and mechanical resonance. Numerical transient flow simulation is an effective front-end engineering measure to assess the susceptibility to detrimental pulsation flow acoustic performance.

This paper reports the simulation results of the discharge flow conditions in a 6-cylinder hexagon shaped reciprocating slurry pump (Hexagonal pump). Two discharge manifold configurations of the same pump are studied comparatively; a case with a hexagon shaped discharge manifold where each cylinder discharges at a single vertex, and a case where all the cylinders discharges are lumped together into a tank shaped manifold. The study establishes the discharge pressure fluctuation characteristics of each configuration, quantifies the flow and pressure pulsation, and decouples the pulsation characteristics of the pump and the discharge manifold.

In addition, the study examines the effect of two pulsation mitigation measures in the case of hexagonal pump with hexagonal manifold; a single inline orifice in one of the hexagon sides and a volumetric dampener at the manifold outlet. Finally, it compares the discharge pulsation characteristics of a reciprocating hexagonal pump with those of similar capacity triplex pumps conventionally used in oil wells drilling and in the mining industry.

A one-dimensional transient flow simulator is used to investigate the pumping hydrodynamic of a slightly-compressible homogeneous slurry flow. The Hexagonal pump analyzed is based on an emerging industrial product design where the vertical reciprocating motion of the pistons is driven by a rotating cam, and where the kinematic of the piston motion is carefully configured, by the cam profile, to smooth the compound pump discharge flow/pressure.

The simulation results of the common discharge tank case show that, under realistic conditions of delays in valves actions, severe discharge pulsation occurs. This pressure pulsation is in the same level of severity as in the crankshaft driven triplex pump used conventionally in drilling oil and gas wells.

Furthermore, the simulations of the hexagonal manifold revealed that a complex alternating flow condition prevails in the six sides of the hexagons in response to the six reciprocating pistons actions. Simulation results suggest that the Hexagonal manifold provides certain level of damping when compared with the case of discharging to a common tank manifold. However, it generates multiple high energy frequency spikes over a wide frequency range, some of them at the high frequency range, with tendencies to excite the piping system and the mechanical frame of the pump.

Received April 12 2013; accepted for publication June 23 2013: Review conducted by Prof. Xuelin Tang. (Paper number O13022C)
Corresponding author: Milan Stanko, Msc., milan.stanko@ntnu.no

2. Introduction

Reciprocating pumps, by the nature of their pistons motion kinematics, experience acceleration and deceleration of the pumped fluid at each pumping cycle. These produce oscillatory variations in flow and pressure at the pump discharge which produce in the fluid a continuous series of propagating compression and expansion zones where fluid particles are vibrating to produce changes of density and pressure along the direction of motion, forming a longitudinal **acoustic compression wave**. These incidental waves are reflected at any acoustic reflector on their propagation path, including a constant pressure node some distance away from the discharge, and return as reflective waves.

Depending on the nature of the waves (amplitude, frequency, phase shift), the interference of the incidental and reflective waves in any point along the flow conduit can be of a **constructive** nature where the waves travelling in the opposite directions are superimposed, and thus their energies are added. They can also be of a destructive nature where a positive and negative amplitudes and thus wave energies cancel each other. In real physical flow system with complex flow path a complex pattern of periodic pressure wave is resulted.

Mathematically, based on Fourier's theorem, a periodic complex wave form can be decomposed to a set of periodic harmonic series (Sine and Cosine forms) each series with a particular frequency and amplitude. This allows computing the distribution of the original wave energy versus the spectrum of frequencies. Frequencies at which the response amplitude is a relative maximum are called resonance frequencies. Complex systems, such as reciprocating pump discharge, where there is a considerable damping or energy loss from cycle to wave cycle, have multiple, distinct, resonant frequencies.

Added complexity to the acoustic conditions occurs when the discharge manifold includes points of restriction, pipe size changes or abrupt change of flow direction. These points caused abrupt momentum reductions producing, in turn, large pressure spikes. These generate a "water hammer" like compression wave that propagates in the sonic velocity away from the exciting pressure point.

One of the main concerns of users and designers of reciprocating pumps is pulsation in the piping of the pumping system. In cases where the fluid exciting coincide with the acoustic resonance and with the piping vibration response, large piping vibrations, noise and possibly breakdown of the pumps and its valves or the pipe and it accessories takes place. The high pressure and rate of process reciprocating pumps, and the severe consequence of piping and pump part breakdown evokes certain industries to issue codes and standards demanding explicitly pulsation design analysis of the pump and the entire pumping system (API Std. 674 [1]). Other industries or applications areas, like mining processing and oil wells drilling, perform only voluntary pulsation analysis depending on the interest of the users or the suppliers.

The first edition of the classic engineering text book titled Hydraulic Transients by Wylie and Streeter published in 1967, and subsequent editions from the same authors with revised titles and upgraded content (Wylie, Streeter, and Lisheng Suo [2]) detail numerical computation approaches to simulate fluid transients and fluid acoustic responses in system of reciprocating pumps categories. In fact, they even listed the codes of many relevant computer programs. Today there is a large body of text and reference books, as well as engineering and scientific papers addressing such computations. There is also a variety of commercial computer programs using variety of numerical approaches (Corbo and Stearns, [3]) , and several consultancies that use their in-house developed software to provide analysis and advices on pump pulsation characteristics.

The intention in this paper is to demonstrate by a simple fluid transient analysis that certain pumps and manifolds configurations under consideration these days and which are loaded with attractive features for the users and the suppliers are prone to severe pulsation. Developments of pulsation prone new pumps and manifold designs call for thorough qualification and verifications programs with regards to their dynamic performance.

No systematic test program has been conducted to substantiate the simulation results of this study. However, references describing a test-bench and a prototype field tests to qualify hexagonal pump for the oil well drilling industry, point at potential of pumping pulsation.

The Hexagonal Reciprocating pump addressed in this paper is a positive displacement axially reciprocating piston pump for heavy duty (high pressure and high rate) slurry pumping in the process and drilling industries. The six piston/cylinder units are distributed in a circular array and configured co-axially. At the end of each cylinder there is a valve block with suction and discharge valves acting along an axis perpendicularly to cylinder axis.

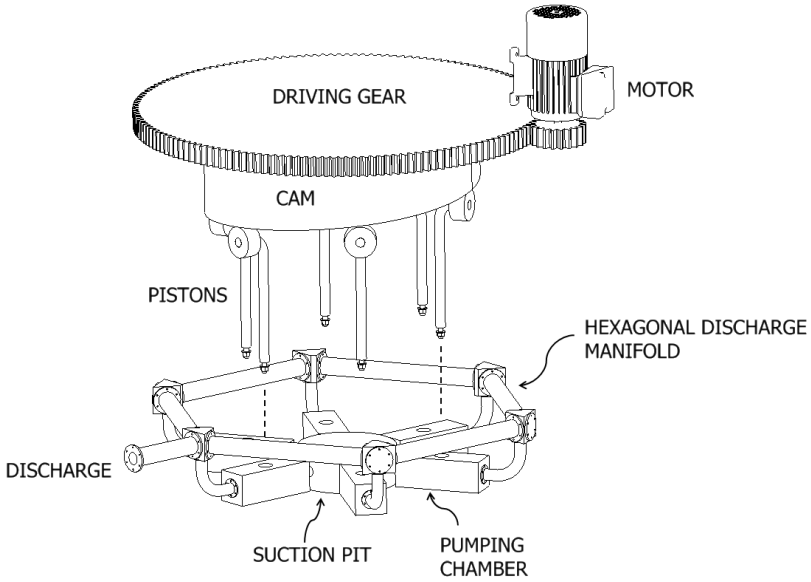

Fig. 1 Schematic configuration of piston assemblies and power end in the hexagonal pump

The axial piston movement is driven by a cam wheel rotating coaxially with the piston motion direction (Fig 1). The profile of the constant speed rotating cam is design to yield a particular piston motion resulting in a ramp-shape discharge pattern (discharge-displacement diagram) with a long rate plateau and a short build-up and decline periods. Furthermore, the compound effect of all the six cylinders, by superposition of the discharge of the individual cylinders, shifted by 60° each will give a smooth and constant compounded discharge rate over a pumping cycle (Fig 2).

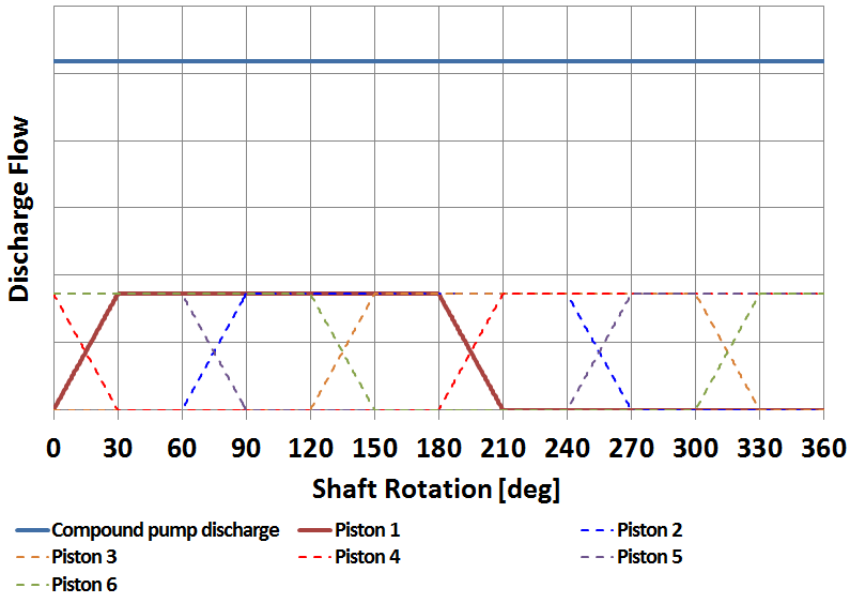

Fig. 2 Discharge flow of the piston used in the hexagonal manifold pump

The compound discharge of all the cylinders is aggregated into a hexagon shaped manifold with relatively small diameter and short length spools connecting the vertexes and where the cylinders discharge are positioned each at a hexagon vertex. The exit of the manifold is at one of the vertexes (fig 3). The suction manifold is a tubular shape tank in the center of the bottom part of the Hexagonal piston array.

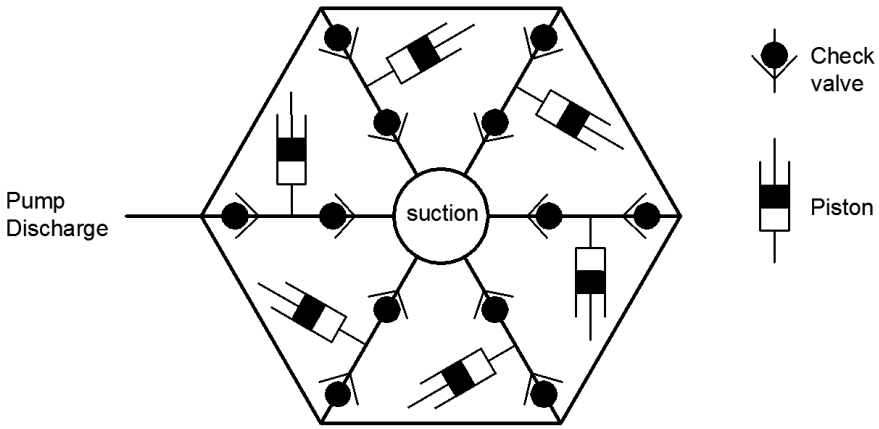

Fig. 3 Pump with hexagonal discharge manifold

Employing a cam wheel to drive the pistons and the hexagonal shaped manifold are new in this category of process slurry pumps. The conventional pumps for this category of application are normally three-cylinder (triplex) pumps where the cylinders are arranged in a parallel manner in a single plane. The pistons are driven by a crankshaft producing a simple harmonic piston motion (SHM or Sinus shape motion). The suction and the discharge manifold are two parallel tube shape (Fig 4 c) where the discharge manifold is normally equipped with a pulsation damper to smooth the rate and pressure fluctuation resulted from the reciprocating motion of the pistons.

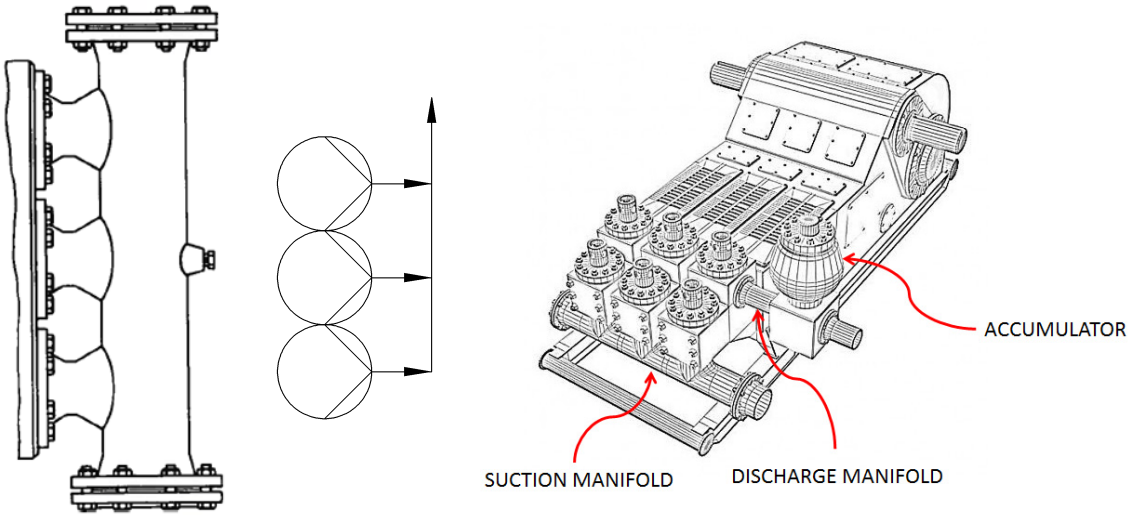

(a) **(b)** **(c)**

Fig. 4 Discharge manifold in reciprocating pumps

The theoretical smooth discharge pressure expected from the 6 piston pump is one of the main drivers for introducing this pump design. However, prototype tests conducted as part of the qualification test (Kverneland et al [4]) gave a few subtle clues that in real operation conditions, with valve action delays and with non-ideal liquids, the pump may develop severe fluctuation. While the novel kinematic of a piston motion and the compounding effect of a six cylinder pump has promised ideally a smooth discharge condition, the interface of the cylinders discharge may excite detrimental pulsation.

This paper examines the discharge pressure of the Hex pump using a transient hydraulic simulator. The study consists of two parts:

- Simulation of the discharge characteristics of the Hex pump and comparison with the characteristics of a Triplex crankshaft driven pump and a six cylinder cam driven pump, both with linear discharge manifold.
- Simulating the pulsation arresting effect of two pulsation reducing measures, a single orifice plat installed on one of the manifold spools and a volumetric dampener conventionally used with triplex pumps.

3. Setting up the simulation cases

The simulated system consists of a pump with a 40 m long horizontal steep pipe tied-in to the discharge side of the pump and with a constant pressure of 300 bara at the exit of the pipe. Three cases, each with different pump, are simulated (Fig 5). The cases are selected as to distinguish between the effects of pump configuration, number of pistons, and the shape of the discharge manifold. In all cases, the pumping rate is 38.5 l/s:

a) Conventional triplex pump-with sine shape, simple harmonic piston motion (crankshaft drive) and with linear manifold

b) Six piston hexagonally arranged pump with ramp type piston motion (rotating cam drive) and with linear discharge manifold

c) Hexagonal pump with ramp type piston motion and with hexagonal discharge manifold

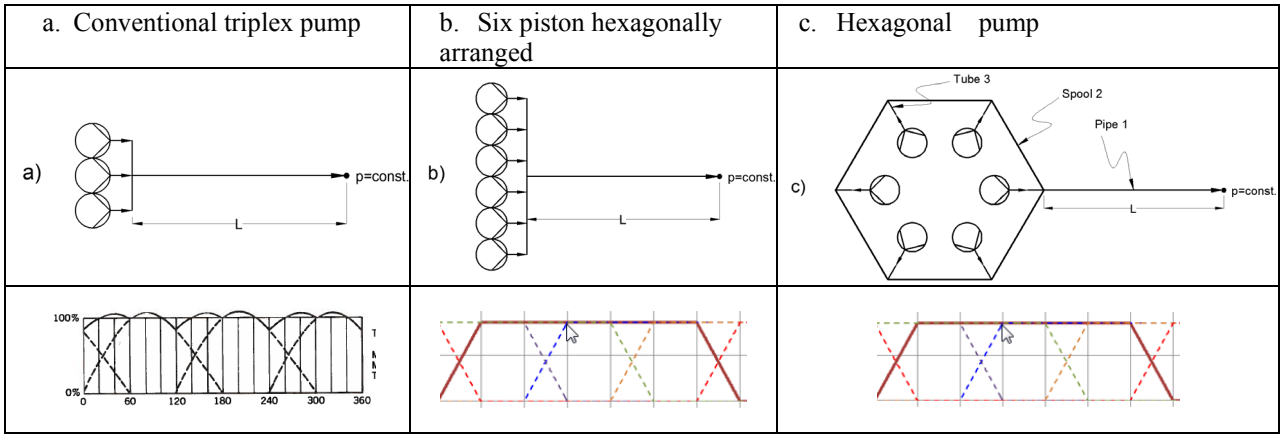

Fig. 5 Cases simulated using transient hydraulics

The relevant fluid and simulated pipe section properties are listed in table 1 and the dimensions of the pipe section and the short spools of the hexagonal manifold are listed in table 2.

Table 1 Fluid properties and pipe properties and characteristics

Fluid properties		**Pipe properties**	
Fluid density [kg/m^3]	1350	Elasticity module [MPa]	203282.4
Fluid viscosity [Pa s]	21e-3	Poisson ratio	0.3
Bulk elasticity module [bar]	20759.4	Pipe support	Anchored upstream
Constitutive fluid model	Newtonian		

Table 2 Piping geometrical characteristics

	Pipe 1	**Spool 2**	**Tube 3**
Length [m]	40.0	1.2	0.3
Inner diameter [mm]	103.2	103.2	80.1
Pipe thickness [mm]	19.1	19.1	17.1

The simulations address two piston kinematics and their associated discharge characteristics

- Ramp shape- Generated by rotating disk-shaped cam
- Sinusoidal profile- generated by crankshaft power end

The real ramp and sinusoidal discharge flow profiles have a distortion or cut out from the ideal curves. These distorted profiles are input to the dynamic flow simulation. The distortions, or cut-outs, are caused by fluid compressibility and by the dynamic of valve motion. The calculations of the distortions are not reported in this paper but their obtained magnitude corresponds to the widely observed and reported in pumps literature. The characteristic of the two considered discharge profiles with and without their considered delays are illustrated in Fig. 6 and their characteristic information is summarized in in table 3.

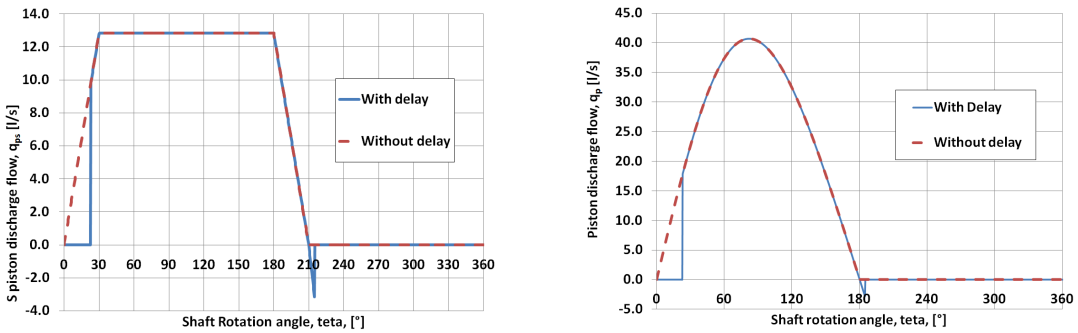

(a) Ramp shape discharge **(b) Sinusoidal shape discharge**

Fig. 6 Ideal and real piston discharge for: (a) Ramp profile, (b) Sinusoidal profile

Table 3 General data for the calculation of the sinusoidal and Ramp piston discharge

Ramp discharge profile		**Sinusoidal discharge profile**	
Maximum flow [l/s]	12.826	Piston diameter [mm]	148.5
Pump speed [RPM]	125	Stroke length [mm]	355.6
Fluid compressibility delay [°]	18	Rod length [mm]	1244.6
Suction valve closing delay [°]	5	Pump speed [RPM]	125
Discharge valve closing delay [°]	5	Fluid compressibility delay [°]	18
		Suction valve closing delay [°]	5
		Discharge valve closing delay [°]	5

4. Setup of the simulations

4.1 The simulator

The simulations in this study were conducted by a simulator for transient flow in a pipe of a homogenous and slightly compressible fluid. It is based on solution of the partial differential equations of the mass and momentum conservation taking into account the fluid and pipe elasticity. The differential equations are converted to ordinary differential equations using the method of characteristics, and these are discretized using finite differences on temporal-spatial grid, given two finite difference formulas each with a characteristic direction where the formula is valid.

The development of the characteristic formulas and the strategy for solving them with the boundary conditions are given in Appendix A. The appendix comments also on the approach to determine a time step for the solution. Time step solution requires special considerations as the pipe and the manifold tubes and spools constitute a piping network with a wide range of pipe length elements, where all of them need to use the same time step in the solution.

The friction factors used in the finite different formulas are the conventional and widely used steady state approximation: Blasius equation for laminar flow and Colebrook correlation for turbulent flow.

All the involved pipes in the network are considered thick walled for their elastic response to inner pressure. The simulated pipe support for each pipe or spool segment is simplified by an upstream anchor (pipe end is fixed in all 3 dimensions).

4.2 The boundary conditions

The boundary conditions used in the solution of the three simulation cases are time-dependent flow at the pump discharge end of the system and a constant pressure at the exit of the 40 m pipe section.

Cases a) and b) have a single point flow boundary conditions at the outlet of the linear shaped and relatively large volume discharge manifold. In case c) there are six point flow boundary conditions representing the individual pistons discharge. This includes the hexagonal discharge manifold in the model.

The input to the simulator is a two column table listing a time series with its corresponding flow for the total time duration of the simulation.

The time dependent flow at the boundary for case a) is calculated by adding three piston discharge rates with an angle shift of 120° between them. The individual discharge of a sinusoidal piston is obtained from the piston velocity expression derived from the time dependent motion of the crankshaft mechanism.

The time dependent flow at the boundary for case b) is calculated by adding six piston discharge rates with an angle shift of 60° between them. The individual piston discharge is calculated with data listed in table 3.

The time dependent flows at the boundary for case c) are calculated by phase shifting 60° the discharge of individual piston by 60°, 120°, 180°,240° and 300°.

The constant pressure boundary at the exit from the 40 m pipe represents a hydraulic element such as a reservoir, tank or a position in the system where the pressure pulsations caused by the pump have dropped to a negligible level. The boundary conditions are summarized in figure 7.

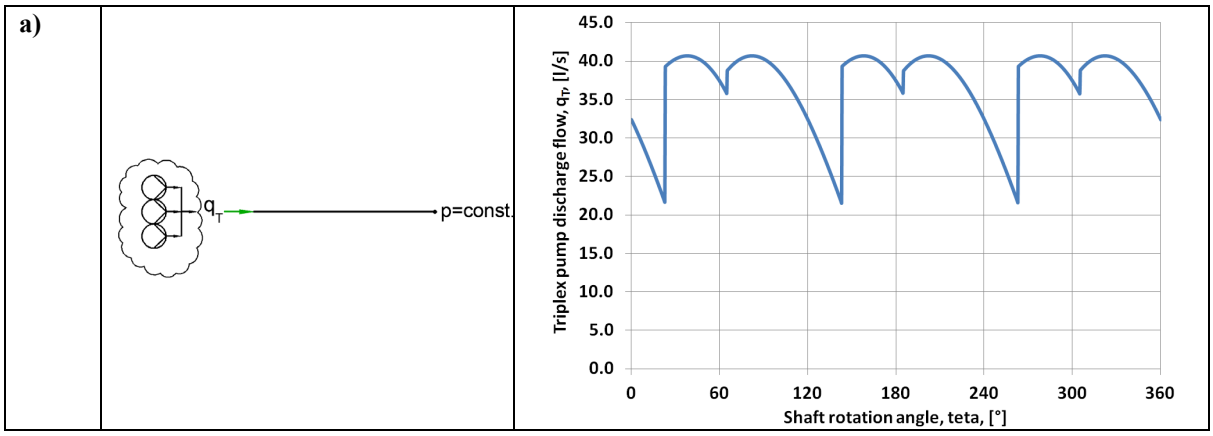

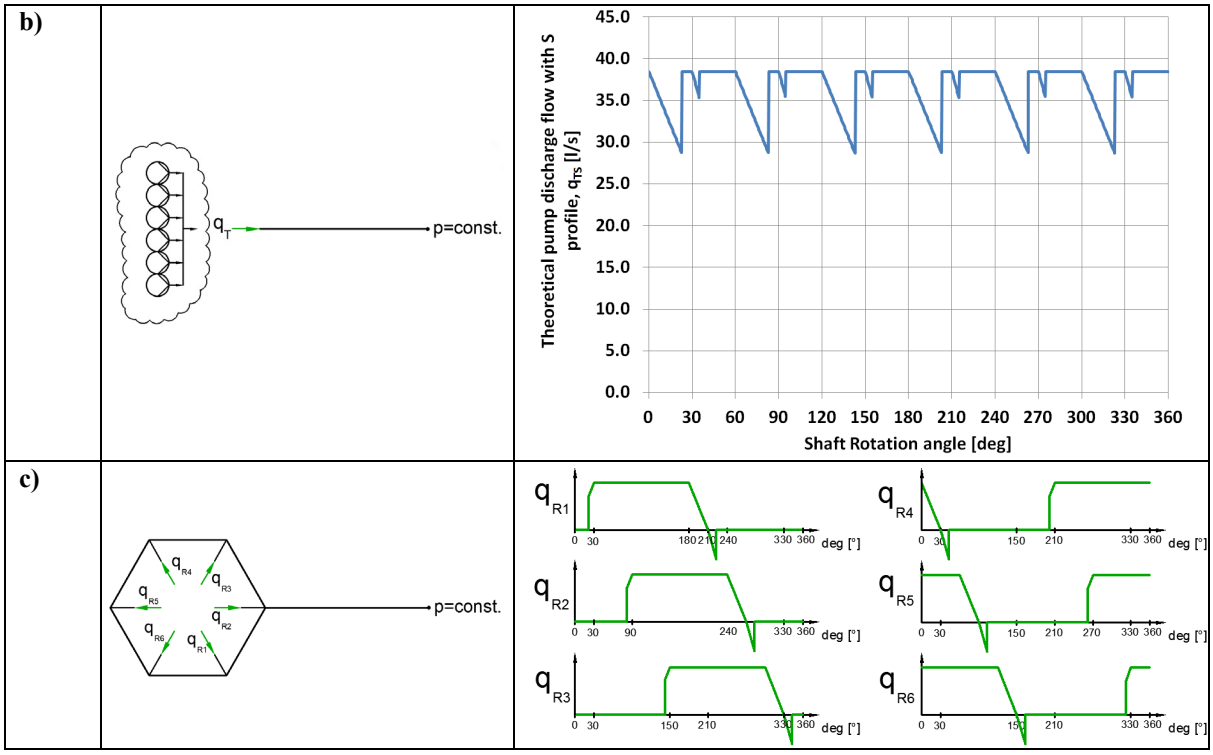

Fig. 7 Time dependent flow boundary conditions for cases a, b and c.

The transient simulations were carried out departing from a steady state solution. The steady state solution for each particular case was calculated by imposing the flow values corresponding to time = 0 s. The transient simulation was performed for a total time of 60 s, and with a time step of 2.49e-4 s.

5. Simplified resonance assessment of the system

The pressure pulsation generator element in the system is the volumetric pump. It excites the discharge pipe by introducing mass periodically which in turns causes a fluid compression or decompression in the boundary. The way the hydraulic system responds to this excitation is computed by solving the discretized momentum and mass fluid conservation equations.

The solution of these set of equations shows that pressure perturbations propagate in the hydraulic system with a wave type motion at a characteristic speed "a". The wave speed "a" depends on the fluid and pipe characteristics. This justifies the employment of analogies from general acoustic theory which are useful to understand the interaction between the wave and the system. The pressure pulsations travel from the pump end to the constant pressure boundary. There are also phenomena such as constructive or destructive superposition and reflection when the pressure waves interact with each other and with the system elements and boundaries. The result is a series of pressure waves travelling in the system with their own distinctive amplitude, frequency and angle shift.

The superposition of all the pressure waves in the system yields a standing wave (or non-moving wave) where the pressure on each point in the system oscillates with a characteristic frequency and amplitude. For very simple acoustic systems it is possible to determine the wave frequency that yields maximum constructive superposition and thus maximum amplitude. This is called the natural frequency of the system. Any multiple of this frequency (called harmonics) yields also the maximum constructive superposition. If an acoustic system is excited with its fundamental frequency or any of its harmonics it is said that the system is in acoustic resonance.

The 40 m long pipe analyzed in the present study has two boundaries: pump and constant pressure. The pressure at the pump end has to change according to the amount of fluid that is being introduced to the system. This corresponds acoustically to a "closed end". The pressure wave is reflected on a closed end like a mirror image: with the same amplitude and frequency.

The constant pressure boundary condition maintains the same pressure without being influenced by the rest of the system. This corresponds acoustically to an "open end". The pressure wave is reflected on an open-end with the same amplitude and frequency but shifted 180°.

This hydraulic system was analyzed acoustically as a closed-end and open-end system. This is perfectly valid for cases (a) and (b) but for case c might be inadequate. The hexagonal manifold is a complex system of interconnected pipes that the current analysis is overlooking.

The fundamental frequency is calculated with eq 1:

$$f = \frac{a}{4 \cdot L} \tag{1}$$

The expected maximum and minimum pressure values for each point of the system for different harmonics is shown in fig. 8. The pressure at each point pulsates with the corresponding harmonic frequency.

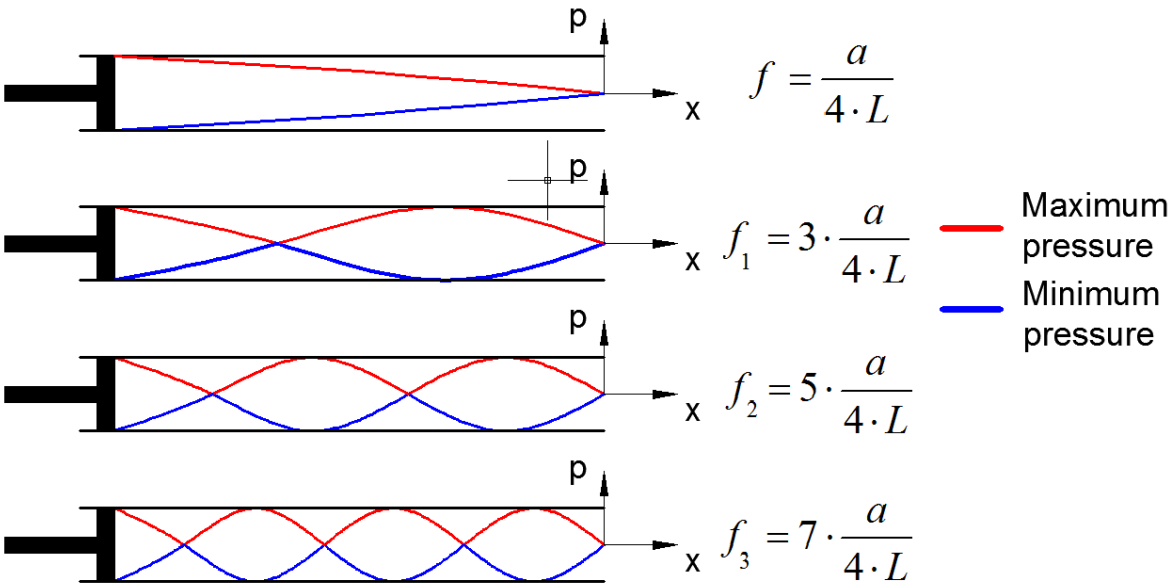

Fig. 8 Resonant mode shapes for an open-closed end pipe**.**

Equation 1 is calculated for cases a, b and c in table 4. The harmonics of these fundamental frequencies are also computed up to number 3. These values constitute the excitation frequencies where resonance is expected.

Table 4 Fundamental frequency and harmonics of the discharge pipe

Case	a/b	c
Wavespeed [m/s]	1200.91	1197.86
Fundamental frequency [Hz]	7.51	7.49
1st harmonic	22.52	22.46
2nd harmonic	37.53	37.43
3rd harmonic	52.54	52.41

The pressure waves/perturbations generated by the volumetric pump are not purely sinusoidal perfect waves. However there is typically a dominant frequency that contains most of the wave energy. This is usually taken as the representative frequency to make the acoustic-like analysis of the system. This frequency is usually dictated by the movement of the shaft.

In the case of a triplex pump there is an excitation 3 times within a shaft revolution and in the case of the hexagonal pump there is an excitation 6 times within a shaft revolution.

The excitation frequencies of the pumps for case a, b and c were computed and are shown in table 5.

Table 5 Excitation frequencies for the studied cases

Case	a	b/c
Shaft speed [RPM]	125	125
Shaft speed [Hz]	2.08	2.08
Base frequency [Hz]	6.25	12.50
2nd harmonic [Hz]	12.50	25.00
3rd harmonic [Hz]	18.75	37.50
4th harmonic [Hz]	25.00	50.00
5th harmonic [Hz]	31.25	62.50
6th harmonic [Hz]	37.50	75.00

In case: a) the pipe is hydraulically excited in its 2nd harmonic, by the 6th pump harmonic. In cases b) and c) the 2nd harmonic of the pipe is hydraulically excited by the 3rd pump harmonic.

6. Results

The transient results of the simulations were inspected visually to discard the stabilization period between the steady state solution and the "stable transient". The "stable transient" is defined when there is qualitative and quantitative repetition of the variables after a time period.

The range selected for the post processing analysis was from 30 to 30.48 s (one period of the pump shaft rotation). Fig. 9 below shows the discharge pressure and flow for cases a, b, c and the maximum, minimum, average and peak to peak values of these two variables.

a)

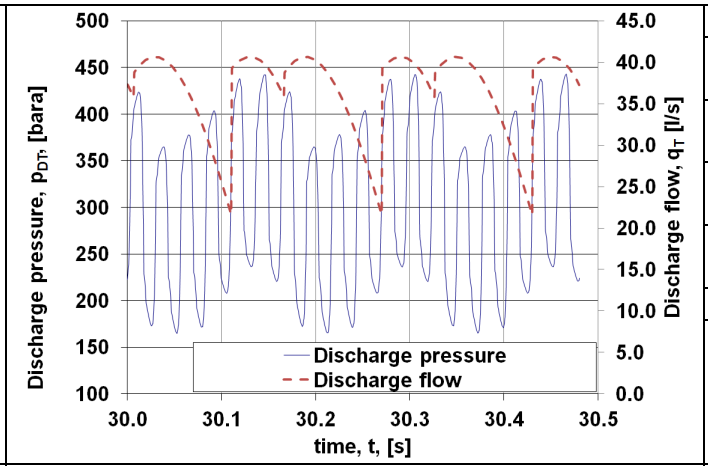

	Pressure	Flow
Max [bara], [l/s]	443.1	40.7
Min [bara], [l/s]	164.6	21.6
Ave. [bara], [l/s]	301.8	36.6
Pk-Pk* [bara], [l/s]	278.6	19.1
Pk-Pk [%]	92.3	52.2

*Pk-Pk: Peak to Peak value

b)

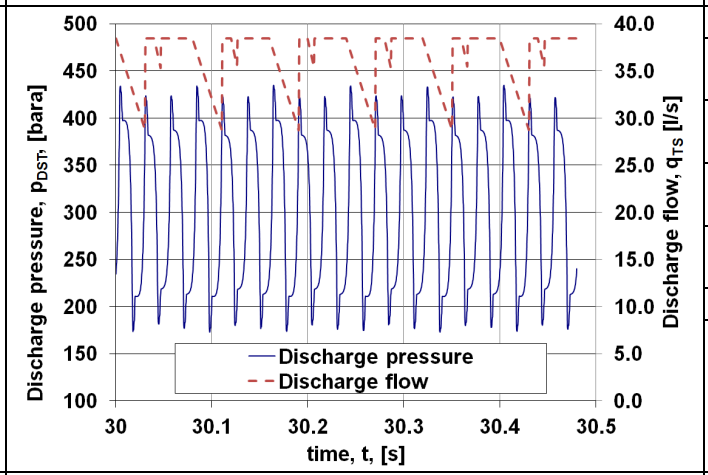

	Pressure	Flow
Max [bara], [l/s]	435.1	38.5
Min [bara], [l/s]	173.1	28.7
Ave. [bara], [l/s]	301.7	36.5
Pk-Pk [bara], [l/s]	262.0	9.8
Pk-Pk [%]	86.8	26.9

c)

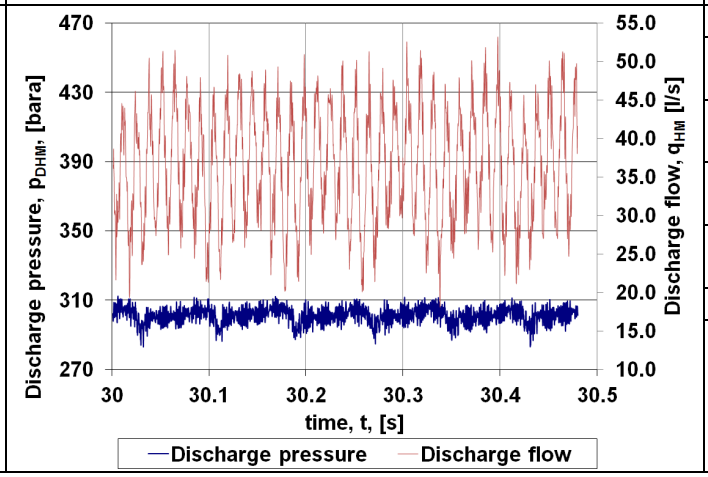

	Pressure	Flow
Max [bara], [l/s]	312.7	53.3
Min [bara], [l/s]	282.1	18.2
Ave. [bara], [l/s]	301.1	36.5
Pk-Pk [bara], [l/s]	30.6	35.2
Pk-Pk [%]	10.2	96.4

Fig. 9 Calculated discharge pressure and flow for one pump period (T = 0.48 s) for cases a, b and c.

The triplex pump (case a) exhibits the most severe discharge pressure fluctuation. The peak to peak values of pressure are 92.3% of the average discharge pressure. The maximum flow corresponds to 11% above the mean and the minimum flow corresponds to 41% below the mean.

The pressure fluctuations of case b have a similar behavior to case a, however, the discharge flow fluctuation band is significantly less than of the triplex pump (max 5% above mean and minimum 21% below mean).

When comparing the flow discharges of cases b and c it is important to note that the presence of the hexagonal manifold creates a discharge flow pattern completely different from the superposition of the individual piston flow discharges. The

hexagonal manifold configuration exhibits the most severe discharge flow fluctuation (maximum 46% above mean and minimum 50% below mean). This flow fluctuation occurs several times within a cycle, at a dominating frequency of 75 Hz, far superior than the theoretical superposition case.

In spite of the flow fluctuations, the pressure fluctuations of case c are the less severe, with a peak to peak value of 10% of the average pressure. The magnitude of the pressure fluctuations are comparable with the values reported in Fig. 2 of the paper by Kyllingstad et al. [5].

6.1 FFT analysis of the pressure results

The discharge pressures of the three cases were processed with Fast Fourier Transform analysis. The time period taken for the analysis was from 30-34 s of data. The calculated frequency spectra are presented in Fig. 10 below.

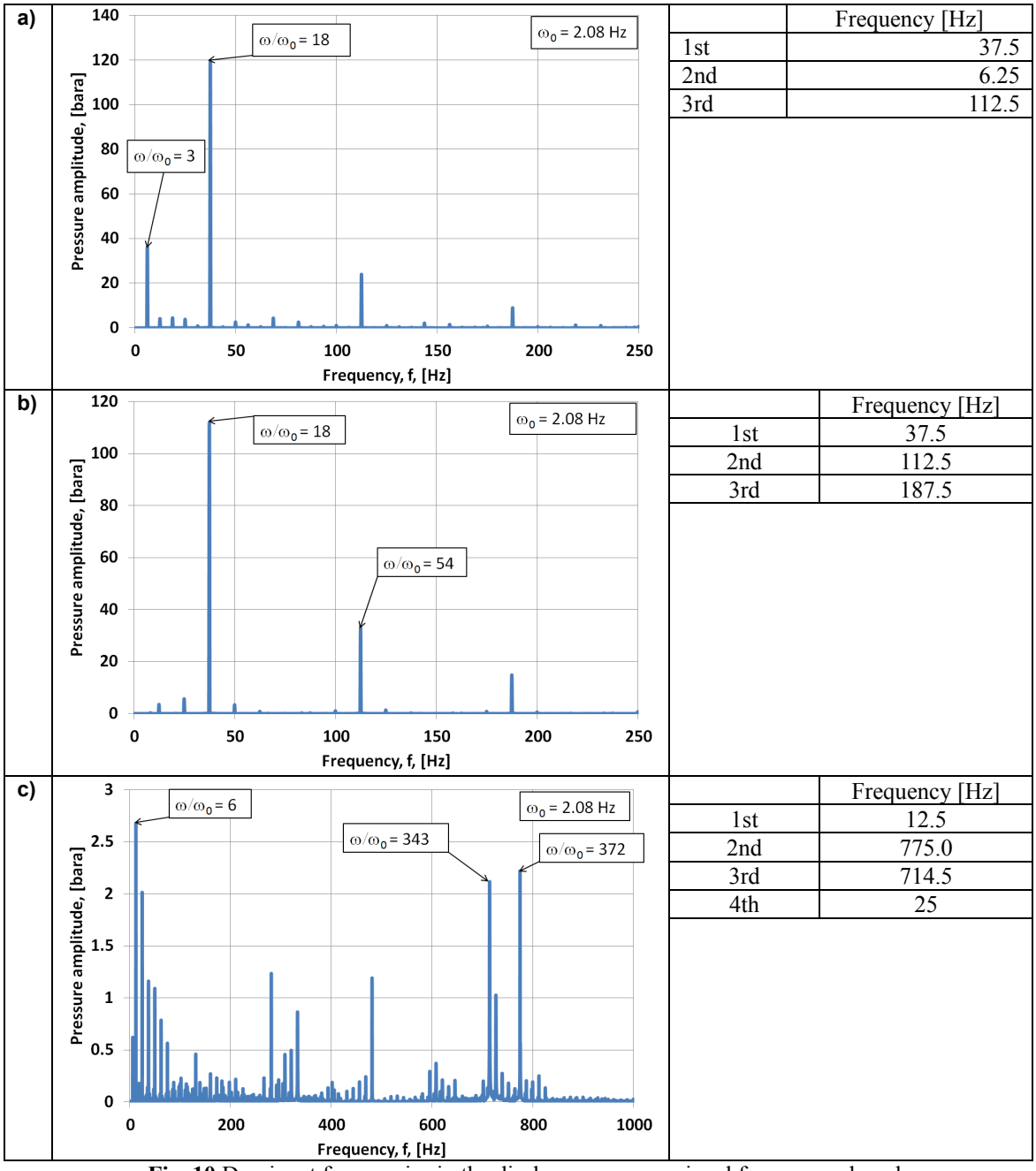

	Frequency [Hz]
1st	37.5
2nd	6.25
3rd	112.5

	Frequency [Hz]
1st	37.5
2nd	112.5
3rd	187.5

	Frequency [Hz]
1st	12.5
2nd	775.0
3rd	714.5
4th	25

Fig. 10 Dominant frequencies in the discharge pressure signal for cases a, b and c.

For cases a) and b) there is one clear frequency that contributes most to the pressure fluctuation signal. The value of these frequencies is 37.5 Hz which corresponds to the 6th (case a) and 3rd (case b) harmonics of the pumps base frequencies.

The frequency spectrum of case c) show several frequencies that make an important contribution to the pressure fluctuation signal. The predominant frequency (with the biggest amplitude) corresponds to the base frequency of the pump (12.5 Hz).

The range of frequencies with relevant amplitude is broader than in cases a) and b), reaching frequencies of 775.0 Hz and 714.5 Hz. These frequencies might be a consequence of the pipe connectors between the piston discharges and the vertexes of the hexagonal manifold.

6.2 Pressure and flow inside the hexagonal manifold

The results of the simulation of case c indicate that there is reciprocating flow in the hexagonal manifold sectors between the discharge points of the individual cylinders. This causes a complex flow with alternating direction in sectors of the hexagonal manifold during a single piston cycle (Fig 11).

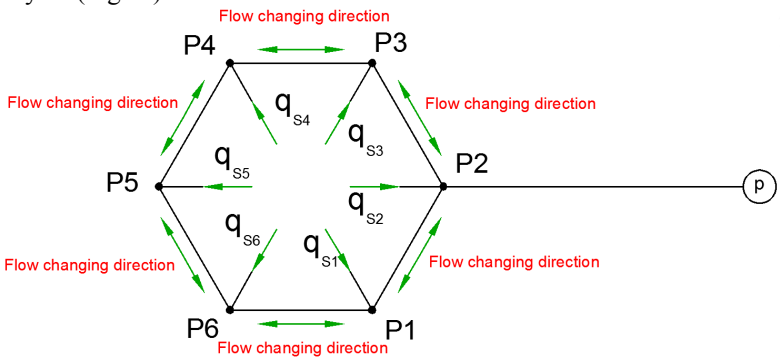

Fig. 11 Diagram indicating the location of alternating flow in the hexagonal manifold.

The alternating flow in the hexagonal ring is not symmetric though the cylinders discharge points are evenly distributed. This is due to the single exit point from the manifold ring that makes the entire flow asymmetric and the sectors flow alternating. As shown in Fig. 12, the most severe changes (alternating intensity) in the flow direction occurs in P5 of the Hex ring, located opposite to the manifold discharge point. Severity of flow direction changes diminish when approaching the hexagonal manifold discharge point.

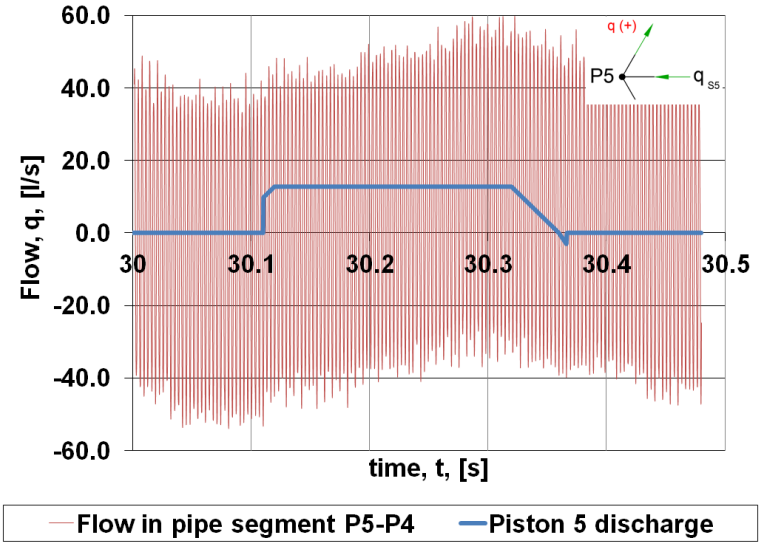

Fig. 12 Reciprocating flow in section P5-P4 of the hexagonal manifold.

The maximum and minimum pressures recorded during the entire simulation time, along the hex ring path P5-P4-P3-P2 are shown in fig. 13. The other branch of the Hexagonal ring (P5-P6-P1-P2) showed a similar behavior. The points of the hexagonal ring with the biggest pressure fluctuation (approx. 200 bar) are located close to P4, P3 and their analogous P6 and P1. The biggest flow fluctuations are the points were the pressure fluctuation is minimum, i.e. P5, between P4 and P3, between P6 and P1 and at the discharge.

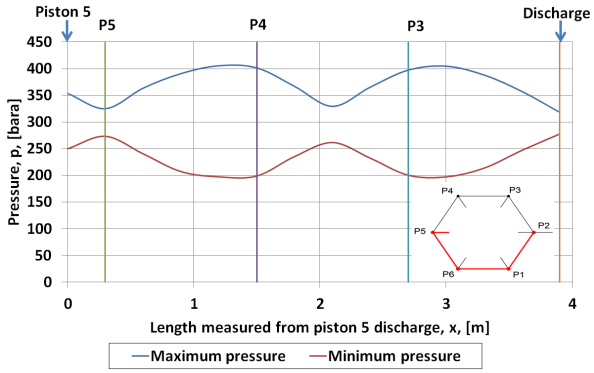

Fig. 13 Maximum and minimum pressure values recorded during the simulation along a branch of the hexagonal discharge manifold.

The maximum and minimum pressure recorded during the entire simulation time, along the discharge piping is shown in fig. 14. The biggest pressure fluctuation does not occur in the pump discharge but at approximately at 4 m, 12 m, 20 m, 28 m and 36 m from the discharge. The graph resembles the fifth mode resonance mode of an open-open end pipe (74.84 Hz).

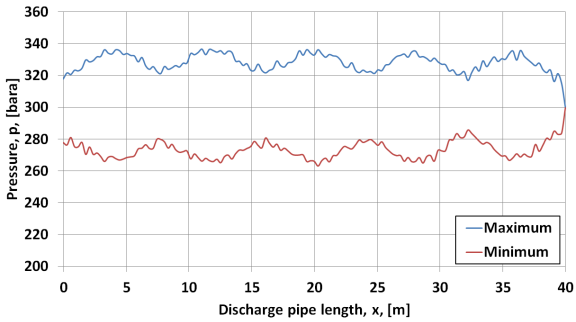

Fig. 14 Maximum and minimum pressure values recorded during the simulation along the discharge piping.

The simulated pressures of the hexagonal manifold points (P1, P3, P4, P5, P6) were processed using FFT analysis for the time range between 30-34 s. Points P1, P3, P4 and P6 showed an identical behavior as the one shown in Fig. 15. The spectra of the pressure signal of point P5 was similar to the one calculated for the pump discharge.

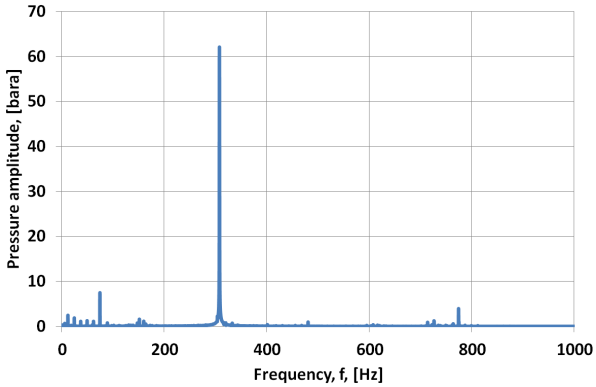

Fig. 15 Dominant frequencies in the pressure signal of the hexagonal manifold point P6.

The existence of a common strong frequency in the pressure signals of points inside the hexagonal manifold could indicate the presence of a high frequency pressure wave that propagates through the hexagonal manifold. This phenomenon could be also aggravated by the circular continuous fluid structure of the hexagonal manifold with low frictional energy dissipation.

7. Pulsation remediation measures

Two measures against pressure pulsation were employed and evaluated for the hexagonal pump: orifice plate and a gas accum ulator. The cases simulated were: 1. hexagonal pump with orifice plate and 2. Hexagonal pump with orifice plate and gas accumul ator

7.1 Hexagonal pump with orifice plate

The orifice plate was placed at 15 cm from P5, on the pipe section that joins P5 and P4 (Fig. 16). This location was chosen because it exhibits maximum flow fluctuation, thus maximizing the dissipative effect of the orifice. The orifice was modeled with a loss coefficient with a value of 577 (approx. 20 bar pressure loss for a flow of 20 l/s through the orifice).

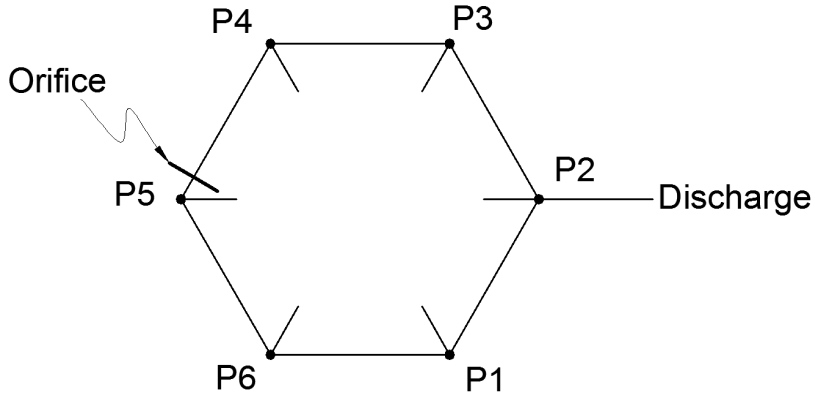

Fig. 16 Hexagonal pump configuration with orifice plate.

The computed discharge pressure and flow are presented in fig. 16 below**.** The magnitude of the peak to peak flow and pressure fluctuations are the similar to those calculated for the original Hexagonal pump. However, the spectra and dominating frequencies of the two signals are different.

1)

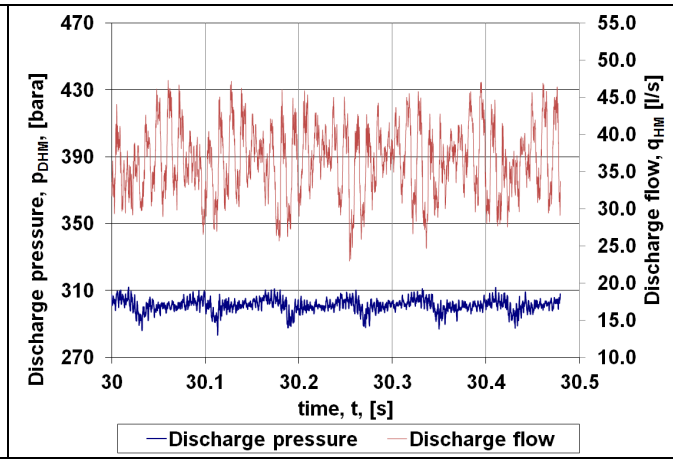

	Pressure	Flow
Max [bara], [l/s]	312.3	47.3
Min [bara], [l/s]	283.3	22.9
Ave. [bara], [l/s]	301.1	36.5
Pk-Pk [bara], [l/s]	29.0	24.4
Pk-Pk [%]	9.6	66.9
Dominating frequency [Hz]	12.5	89.5

Fig. 17 Discharge pressure and flow for the hexagonal pump with orifice.

The main differences between the hexagonal pump with and without orifice are in the hexagonal manifold. The orifice reduces considerably the peak to peak value of pressure pulsation in the manifold from 200 bar to 30 bar (Fig. 18).

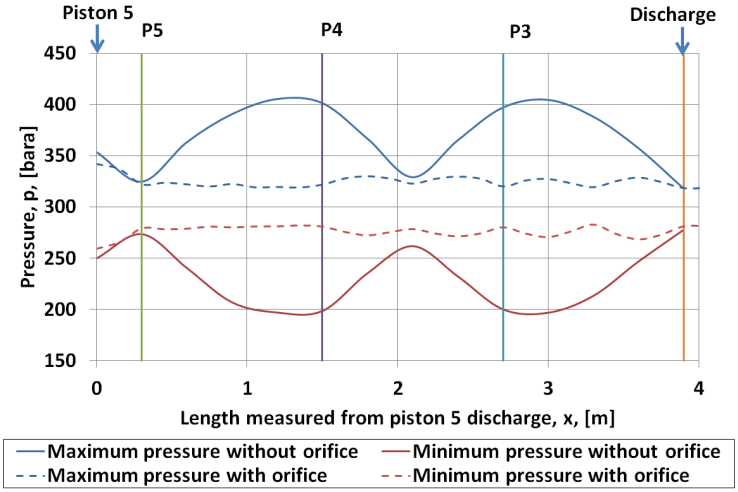

Fig. 18 Discharge pressure and flow for the hexagonal pump with orifice.

The orifice plate has an isolating effect between the two hexagonal manifold branches P5-P4-P3-P2 and P5-P6-P1-P2. This is observable in fig. 19 where the flow in pipe section P5-P4, just after the orifice plate, is graphed for a piston cycle and compared with the discharge of piston 5.

As shown in Fig. 19, the alternating intensity in the flow direction in P5 of the Hex ring has diminished considerably in comparison to the original configuration (Fig. 12). The peak values have a maximum magnitude of 10 l/s while for the original geometry had a value of 60 l/s. The behavior of this flow is dictated roughly the discharge of piston 5, with a positive flow value (from P5-P4) when the piston is discharging and a negative flow value when the piston 5 is in the suction phase.

The orifice diminishes the severity of flow direction changes in the rest of pipe section in the hexagonal manifold, forcing the flow to move towards the discharge.

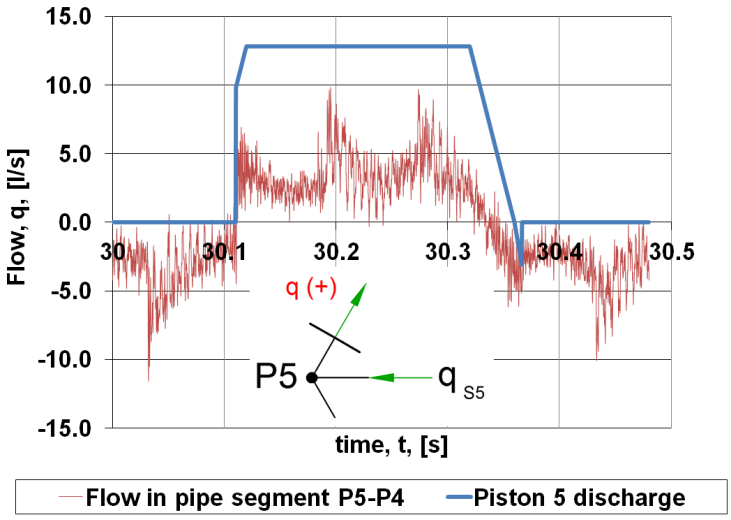

Fig. 19 Reciprocating flow in section P5-P4 of the hexagonal manifold with orifice plate installed.

7.2 Hexagonal pump with orifice plate and gas accumulator

A gas accumulator was placed at the discharge piping of the pump (1 m after the point P2) as presented in fig 20. The accumulator chosen was a 20 gallons pneumatic dampener with nitrogen charge (polytropic coefficient n=1.2). The precharge pressure was set to 242.3 bara. The accumulator is assumed to be connected directly to the pipe with no hydraulic loss.

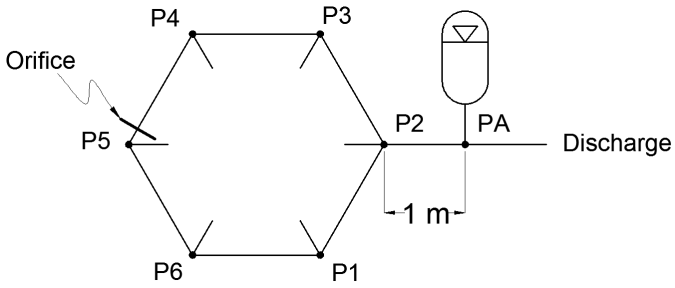

Fig. 20 Hexagonal pump configuration with orifice plate and gas accumulator.

The computed discharge pressure and flow are presented in fig. 21 below**.** The magnitudes of the peak to peak flow and pressure fluctuations have decreased dramatically with the employment of the gas accumulator.

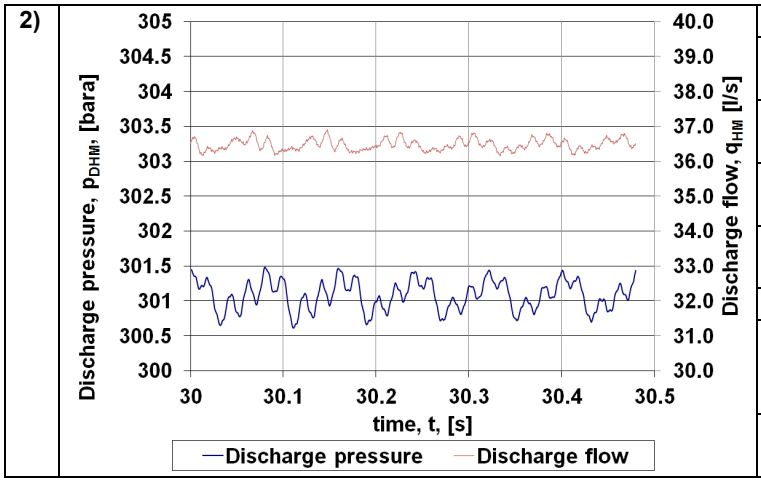

	Pressure	Flow
Max [bara], [l/s]	301.5	36.9
Min [bara], [l/s]	300.6	36.2
Ave. [bara], [l/s]	301.1	36.5
Pk-Pk [bara], [l/s]	0.9	0.7
Pk-Pk [%]	0.3	2.1
Dominating frequency [Hz]	12.5	12.5

Fig. 21 Discharge pressure and flow for the hexagonal pump with orifice and gas accumulator.

8. Conclusions

The hexagonal manifold discharge configuration impedes the superposition of the individual piston flow discharges. The main reason for this is that it causes a complex interaction between the piston's discharges and the flow in the pipe sections.

The hexagonal manifold generates the appearance of multiple dominant frequencies in the discharge pressure signal. Some of these pressure fluctuations occur at much higher frequencies than typical multiplex pumps (around 350 times the shaft rotation frequency for the simulated case). Usually the amplitudes of such frequencies must be limited to avoid the excitation of structural and piping supports.

The delays in the piston cycle (i.e. the volumetric efficiency) are important parameters that have to be accounted for in the modeling of reciprocating pumps.

The pressure pulsation generated by a hexagonal pump configuration (peak to peak fluctuation is 10 % of average discharge pressure) is significantly less than the one produced by a linear superposition of the pistons discharges (peak to peak fluctuation is 87% of average discharge pressure). This indicates that the hexagonal manifold provides certain level of dampening against pressure pulsations.

Due to the high levels of pressure pulsation detected in all the analyzed systems, the need of installation of a pulsation dampening device is mandatory.

The orifice plate improves significantly the pressure and flow fluctuation in the hexagonal manifold (from peak to peak fluctuation of 67% of average discharge pressure to 10%). However it doesn't improve the pressure pulsation levels downstream the pump.

The installation of a 20 gal gas pulsation dampener in addition to the orifice plate reduced dramatically the discharge pressure pulsation levels (discharge peak to peak fluctuation from 10% of average pressure to 0.3%). The resulting configuration however has a bigger footprint than the original Hexagonal pump.

Nomenclature

a ….fluid wavespeed, [m/s]
D ….Pipe inner diameter, [m]
f ….Friction factor [unitless]
g ….Gravitational acceleration [m/s^2]
n….Gas Polytropic Coefficient
p ….Pressure [bara]
t ….time [s]
V ….Fluid velocity [m/s]
x ….Position coordinate, [m]
α ….Pipe inclination angle from the horizontal [rad]
ρ ….Fluid density [kg/m^3]

References

[1] API Std 674, "Positive Displacement Pumps-Reciprocating," (Section 3.6.2) American Petroleum institute, 2nd edition, June 1993.

[2] Wylie, E.B., Streeter, V.L., Lisheng S., 1993, "Fluid Transients in Systems," 8th edition, Prentice Hall.

[3] Corbo, M. A. and Stearns, C. F., 2005, "Practical Design Against Pump Pulsations," Proceedings of the 22nd International Pump Users Symposium, Turbomachinery Laboratory, Texas A&M University, pp. 137-177.

[4] Kverneland, H., Kyllingstad, Å., Moe, M., 2003, "Development and Performance Testing of the Hex Mud Pump," Paper SPE/IADC 79831 presented at the SPE/IADC Drilling Conference, Amsterdam, Netherlands.

[5] Kyllingstad, Å., Nessjøen P., 2011, "Condition based maintenance: A new early leak Detection system for mud pumps," Paper SPE/IADC 139888 presented at the SPE/IADC Drilling Conference, Amsterdam, Netherlands.

Appendix A: Transient fluid dynamics numerical simulator

The numerical tool employed in the present study is a simulator for the analysis of unsteady flow of liquids in piping networks. It is based in the transient conservation equations of mass (A-1) and momentum (A-2), taking into account the fluid and pipe elasticity.

$$a^2 \cdot \frac{\partial V}{\partial x} + \frac{1}{\rho} \cdot \frac{\partial p}{\partial t} = 0 \tag{A-1}$$

$$\frac{\partial p}{\partial x} + \rho \cdot \frac{\partial V}{\partial t} + \rho \cdot g \cdot \sin(\alpha) + \frac{\rho \cdot f \cdot V \cdot |V|}{2 \cdot D} = 0 \tag{A-2}$$

The partial differential equations (A-1) and (A-2) are converted to 2 ordinary differential equations (A-3 and A-5) using the method of the characteristics. Each equation however is valid only for the positions and times that comply with conditions (A-4) and (A-6) respectively.

$$+\frac{1}{\rho \cdot a}\frac{dp}{dt} + \frac{dV}{dt} + g \cdot \sin(\alpha) + \frac{f \cdot V \cdot |V|}{2 \cdot D} = 0 \tag{A-3}$$

$$\frac{dx}{dt} = a \tag{A-4}$$

$$-\frac{1}{\rho \cdot a}\frac{dp}{dt}+\frac{dV}{dt}+g\cdot\sin(\alpha)+\frac{f\cdot V\cdot|V|}{2\cdot D}=0 \tag{A-5}$$

$$\frac{dx}{dt}=-a \tag{A-6}$$

Equations A-3, A-4, A-5 and A-6 were discretized using finite differences on the temporal-spatial grid shown in Fig. A-1 below. The resulting equations are presented below: A-7, A-8, A-9, A-10.

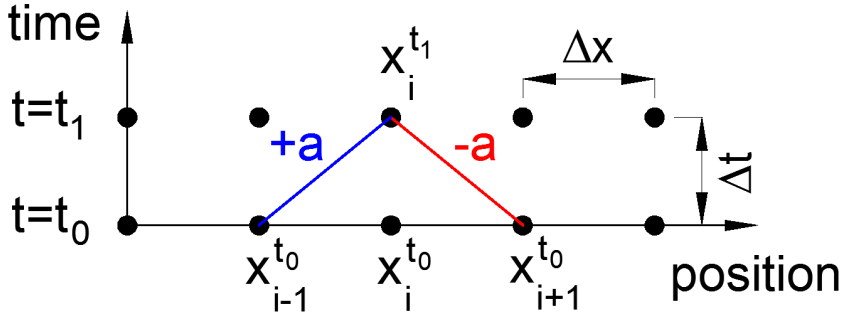

Fig. A-1. Temporal and spatial discretization used in the characteristics method

$$p_i^{t_1}-p_{i-1}^{t_0}+\rho\cdot a\cdot\left(V_i^{t_1}-V_{i-1}^{t_0}\right)+\rho\cdot g\cdot\sin(\alpha)\cdot\Delta x+\frac{\rho\cdot f\cdot V_i^{t_1}\cdot\left|V_{i-1}^{t_0}\right|\cdot\Delta x}{2\cdot D}=0 \tag{A-7}$$

$$\frac{\Delta x}{\Delta t}=+a \tag{A-8}$$

$$+p_{i+1}^{t_0}-p_i^{t_1}+\rho\cdot a\cdot\left(V_i^{t_1}-V_{i+1}^{t_0}\right)+\rho\cdot g\cdot\sin(\alpha)\cdot\Delta x+\frac{\rho\cdot f\cdot V_i^{t_1}\cdot\left|V_{i+1}^{t_0}\right|\cdot\Delta x}{2\cdot D}=0 \tag{A-9}$$

$$\frac{\Delta x}{\Delta t}=-a \tag{A-10}$$

For the inner points of the pipe eq. A-7 and A-9 can be combined to obtain the solution for time t1. For the boundary nodes upstream of the pipe, eq A-9 has to be used in combination with the boundary condition. For boundary nodes downstream of the pipe eq. A-7 has to be used in combination with the boundary condition.

The friction factor was calculated by using the steady state approximation (Blasius for laminar flow and Colebrook correlation for turbulent flow).

All the existing pipes where considered supported as anchored upstream and thick-walled.

In pipe network systems the time step Δt has to be the same for each pipe section "j". The time step is calculated for each pipe section "j" according to equation (A-11) below. Due to the fact that the wavespeed a_j and length L_j are *a priori* different for each section, it is very unlikely that an adequate integer number of subdivisions N_j will be found to achieve an unique Δt. In order to achieve a common Δt the wavespeed in each section was modified slightly (±2%).

$$\Delta t=\frac{L_j}{N_j\cdot a_j} \tag{A-11}$$